Electronic Supplementary Information

Lead Selenide Quantum Dots and Carbon Dots Amplify Solar Conversion Capability of a TiO_2/CdS Photoanode

Ramesh K Kokal,[a] P. Naresh Kumar,[b] Melepurath Deepa,[a,*] Avanish Kumar Srivastava[b]

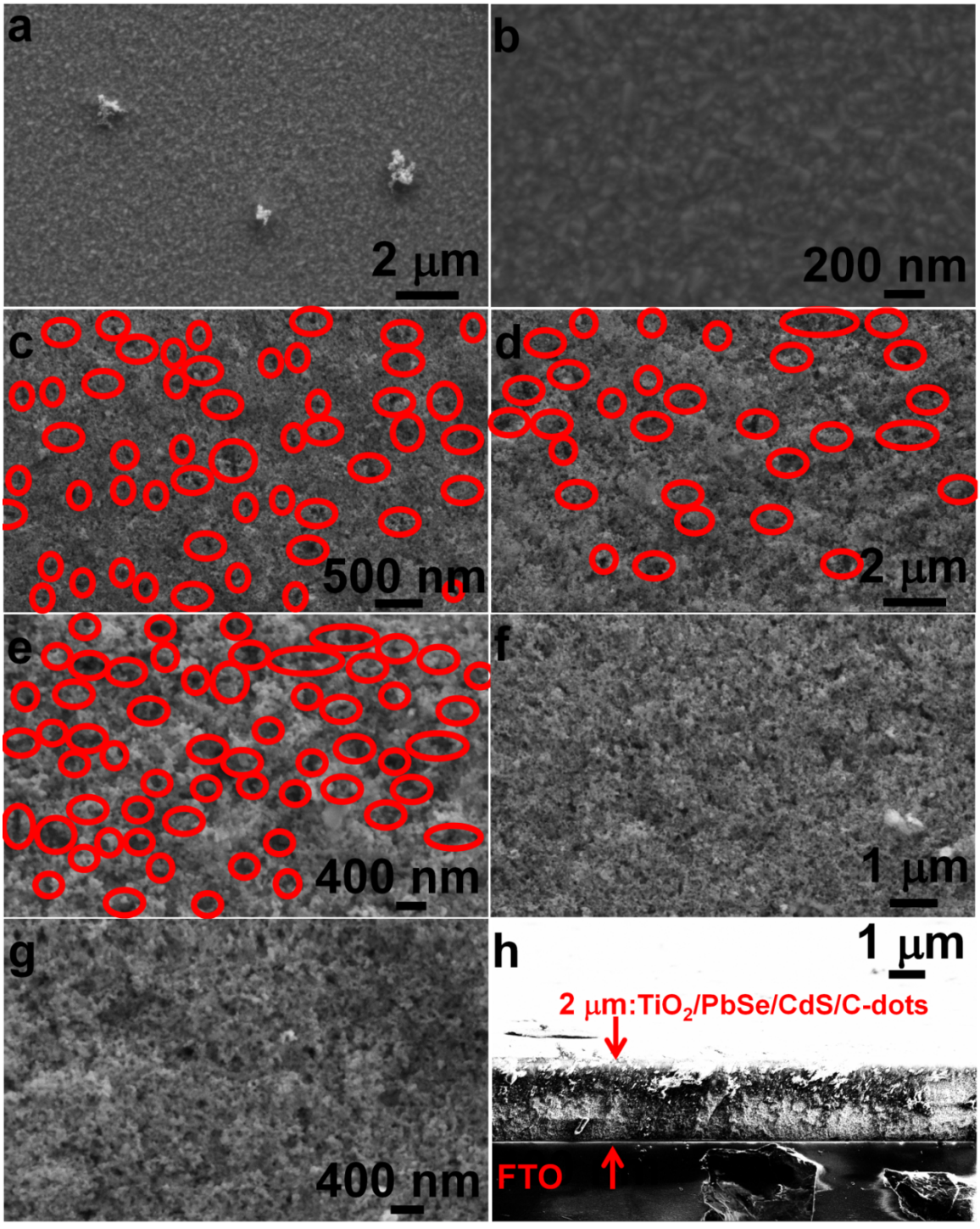

Figure S1 FE-SEM images of (a) and (b): pristine C-dots at different magnifications, (c): a pristine TiO_2 electrode, (d) and (e): a TiO_2/PbSe/CdS electrode at different magnifications, (f) and (g): a TiO_2/PbSe/CdS/C-dots electrode at different magnifications, (h): a cross-sectional view of the TiO_2/PbSe/CdS/C-dots electrode illustrating the film thickness. The red colored solid ellipses in (c) to (e) enclose the pores present in the films.

The X-ray diffractograms of pristine- TiO_2, CdS, PbSe and C-dots are shown in Figure S2. The XRD pattern of pristine TiO_2 shows peaks at d = 3.51, 2.42, 2.37, 1.88, 1.69, 1.66, 1.48, 1.26 Å which correspond to the (101), (103), (004), (200), (105) (211), (204) and (215) planes of the tetragonal symmetry of body centered cubic lattice, in concurrence with the JCPDS card # 89-4921. The XRD pattern of CdS QDs grown on a glass plate by a SILAR process shows a broad peak at d = 3.37 Å and a weak peak at 2.06 Å and these are assigned to the (111) and (220) reflections of the face centered cubic (fcc) lattice of CdS (JCPDS card # 65-2887). The broadness of the peaks indicates a semi-crystalline nature of the CdS QDs. For PbSe QDs, three distinct peaks at inter planar spacings of 3.53, 3.06 and 2.16 Å, followed by weak peaks at d = 1.84, 1.76, 1.53, 1.40, 1.36, 1.24 Å were observed and these match with the (111), (200) and (220), (311), (222), (400), (420) and (422) planes of the cubic phase of PbSe as per JCPDS card # 06-0354. For pristine C-dots, a very broad peak centered at $\sim 2\theta = 26.2^{o}$, d = 3.4 Å, corresponding to the (002) plane of graphitic carbon is observed (JCPDS card # 75-1621). Faint shoulders at $2\theta = 43^{o}$ and 60.1^{o} are also seen, and these agree with the (101) and (103) planes of carbon with a hexagonal unit cell.

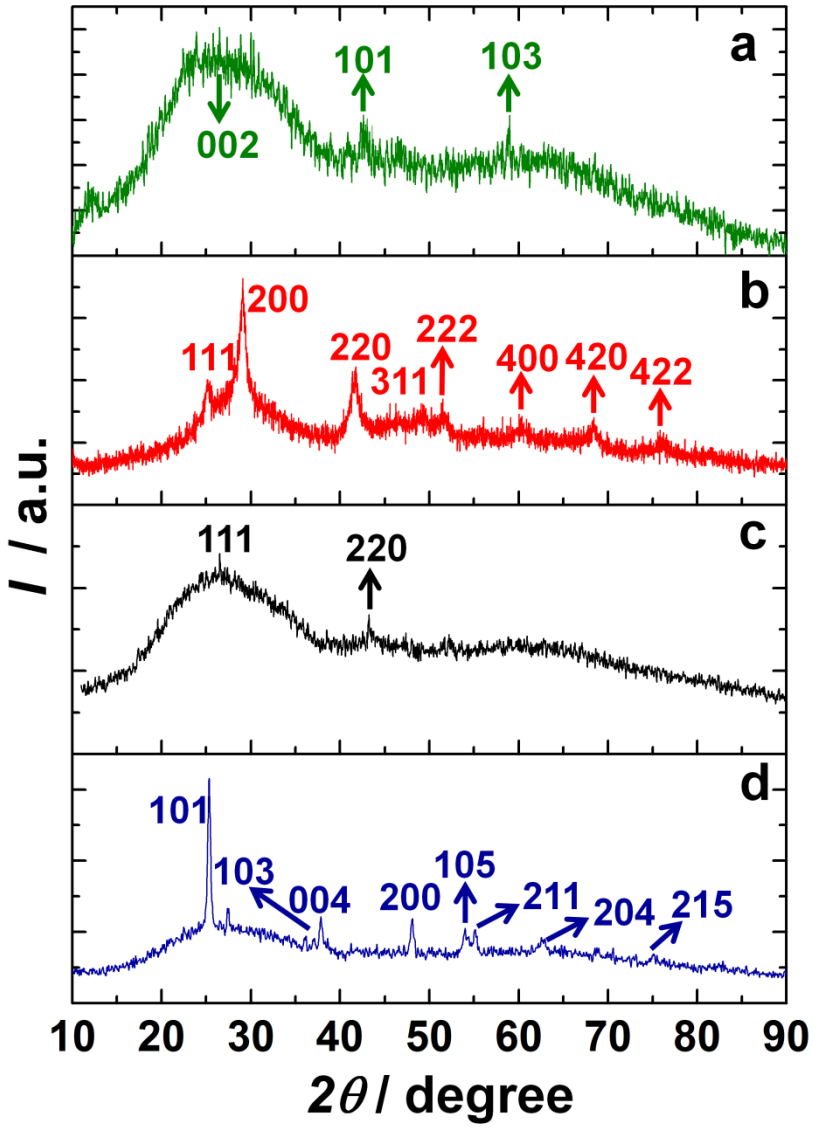

Figure S2 XRD patterns of pristine samples: (a) C-dots, (b) PbSe QDs, (c) CdS QDs and (d) TiO_2.

The Raman spectrum of pristine C-dots (Figure S3a) shows two peaks at 1351 and 1575 cm^{-1}, corresponding to the D and G bands respectively. The D band corresponds to defects, structural imperfections caused by the covalent attachment of oxygen containing groups to graphite and edge areas of graphitic sheets, and this is due to the smaller dimensions of C-dots, compared to graphene sheets. The G band arises from the stretching vibrations of the sp^2 hybridized carbon atoms. The I_D/I_G ratio was calculated to be 0.415. The low value of the D band to G band ratio, is indicative of a low proportion of defects in the graphitic structure, which implies that C-dots are largely composed of sp^2-bonded carbon atoms. The preservation of the graphitic structure can

lead to a high electrical conductivity, which in turn is beneficial for fast electron propagation in the photoanode during operation. I-V characteristics of C-dots were measured by compressing C-dots between two stainless steel electrodes (Figure S3b). The I-V characteristics were recorded between –1 and +1 V, and the dependence is almost linear in the bulk of this potential window, indicating an Ohmic dependence. From the straight line fit, the slope was calculated to be 0.49 Ω^{-1}, and using the relation: σ = Slope (I/V or 1/R) × l/a, where 'l' is the thickness of the sample and 'a' is the active electrode area, the conductivity (σ) of C-dots was determined to be 0.125 S cm^{-1}. This was reaffirmed by an ac impedance measurement. The Z'' versus Z' plot for pristine C-dots is shown as an inset of Figure S3b. The point of commencement of the arc on the abscissa corresponds to the bulk resistance of the sample ($Z'_{C\text{-dots}}$ = R = 2.1 Ω). From the above expression, the conductivity from the Nyquist plot was estimated to be 0.122 S cm^{-1}. The conductivity values from I-V and ac impedance agree well.

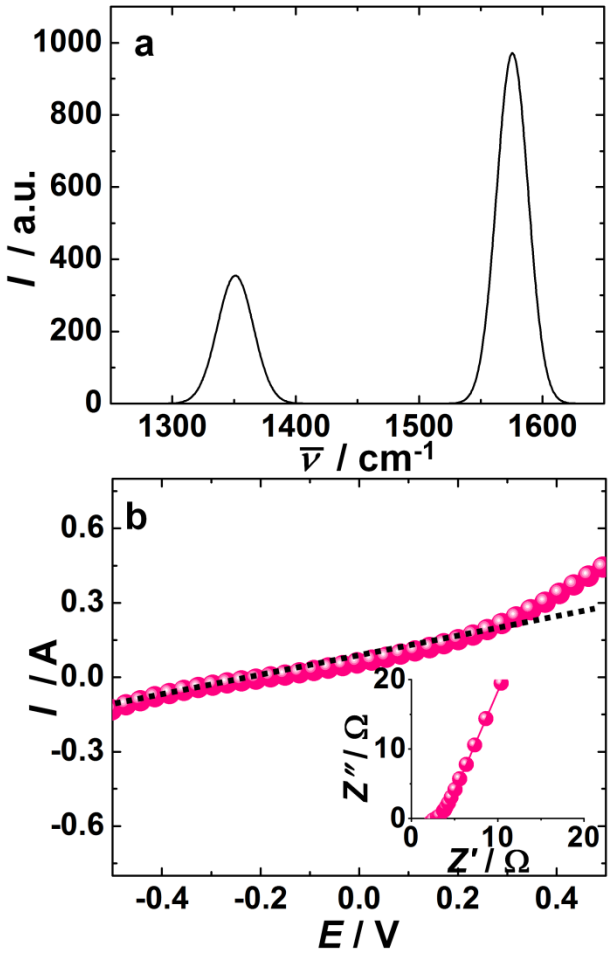

Figure S3 (a) Raman spectrum and (b) I-V characteristics of pristine C-dots. Inset of (b) is the impedance plot of C-dots.

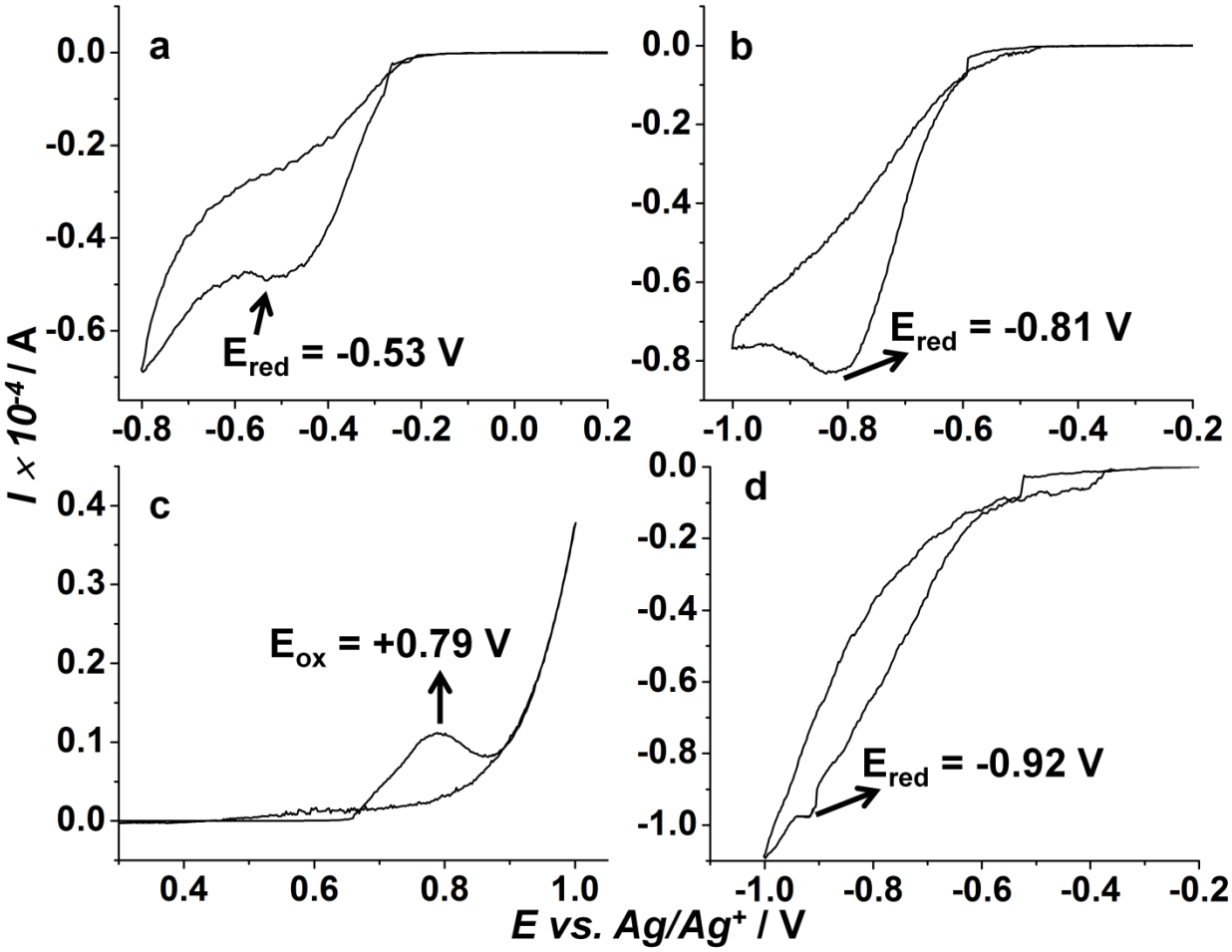

Figure S4 Cyclic voltammograms of (a) a pristine TiO_2 electrode, (b) a pristine CdS electrode, (c) a PbSe electrode, and (d) a C-dots' electrode serving as working electrodes. All CV plots were recorded in a 0.1 M KCl solution as electrolyte, with a Pt sheet as the counter electrode and an Ag/AgCl/KCl as the reference electrode, at a scan rate of 10 mV s^{-1}.

Table S1 Kinetic parameters of emission decay analysis of photosensitizer films deduced from double exponential fits; the λ_{ex} was fixed at 370 nm for all samples.[a]

Sample	λ_{em}	B_1	τ_1 (ns)	B_2	τ_2 (ns)	$\langle\tau\rangle$ (ns)	χ^2
CdS	530	100	11.53	-	-	11.53	1.02
C-dots	440	100	5.10	-	-	5.10	1.06
CdS/C-dots	530	97.32	0.0046	2.68	14.00	13.83	0.98
	440	7.53	0.18	92.47	2.14	2.10	0.95
TiO_2/CdS	530	87.01	0.0062	12.99	1.53	1.40	0.99

TiO_2/C-dots	440	21.25	0.535	78.75	2.91	2.70	0.99
TiO_2/CdS/C-dots	530	97.49	0.00625	2.51	0.54	0.37	1.01
	440	98.08	0.0062	1.92	1.32	1.00	1.1
TiO_2/PbSe/CdS/C-dots	530	8.60	0.00618	91.4	0.147	0.14	0.96
	440	14.39	0.00622	85.61	0.24	0.23	1.1

[a]B is the relative amplitude of each lifetime, τ_1 and τ_2 are the components of fluorescence lifetime and χ^2 denotes the fit quality.

Cyclic voltammograms of pristine- TiO_2, CdS and PbSe films (as working electrodes), recorded in an aqueous 0.1 M KOH solution, with a Pt rod as the counter electrode and a Ag/AgCl/KCl as the reference electrode are shown in Figure S4. For pristine TiO_2, a reduction peak was observed in the cathodic sweep at –0.53 V *versus* Ag/AgCl/KCl, and this E_{red} can be equated to the conduction band (CB) or LUMO (lowest unoccupied molecular orbital) position of TiO_2. The electrode potential of the reference is +0.197 V. So, E_{red} (*versus* NHE (normal hydrogen electrode)) of TiO_2 = –0.53 V + 0.197 V = –0.333 V. The value of –0.333 V (*versus* NHE) in eV is given by: –4.5 eV (≅ 0 V *versus* NHE) – (–0.333V) = –4.167 ≅ –4.17 eV. The position of the valence band (VB) or HOMO (highest occupied molecular orbital) of TiO_2 is determined by addition of the pre-determined optical band gap energy value to the CB energy, i.e., –4.17 eV + (–3.16 eV) = 7.33 eV. For pristine CdS, a reduction peak was observed in the cathodic sweep at –0.81 V *versus* Ag/AgCl/KCl, and this E_{red} can be equated to the CB or LUMO position of CdS. So, E_{red} (*versus* NHE) of CdS = –0.81 V + 0.197 V = –0.613 V. The value of –0.613 V (*versus* NHE) in eV is given by: –4.5 eV – (–0.613V) = –3.887 ≅ –3.9 eV. By adding the optical E_g of CdS to the CB energy level (–3.9 eV + (–2.25 eV)), the VB energy level is calculated to be at 6.15 eV. For pristine PbSe, an oxidation peak was observed in the anodic sweep at +0.79 V *versus* Ag/AgCl/KCl, and this E_{ox} can be equated to the VB or HOMO position of PbSe. So, E_{ox} (*versus* NHE) of PbSe = +0.79 V + 0.197 V = +0.984 V. The value of +0.984 V (*versus* NHE) in eV is given by: –4.5 eV – (+0.984 V) = –5.484 ≅ –5.48 eV. The position of the CB or LUMO of PbSe is determined by the subtraction of the optical band gap energy value from the VB energy (–5.48 eV –(–1.62 eV)) and it is found to be 3.86 eV. For pristine C-dots, a reduction peak was observed in the cathodic sweep at –0.92 V *versus* Ag/AgCl/KCl, and this E_{red} can be equated to the CB or LUMO position of C-dots. So, E_{red}

(*versus* NHE) of C-dots = –0.92 V + 0.197 V = –0.723 V. The value of –0.723 V (*versus* NHE) in eV (*versus* vacuum) is given by: –4.5 eV – (–0.723 V) = –3.777 ≅ –3.78 eV.

Table S2 Solar cell parameters of cells by considering standard deviation using 0.1 M Na_2S electrolyte, exposed cell area: 0.12 to 0.15 cm^2, under 1 sun illumination (AM 1.5G, 100 mW cm^{-2}) with the listed photoanodes; all cells with MWCNTs as the counter electrode.

Photoanode	V_{OC} (mV)	J_{SC} (mA cm^{-2})	FF	η (%)
TiO_2/CdS	704.45 ± 15.25	7.82 ± 0.26	44.25 ± 0.10	2.44 ± 0.14
TiO_2/PbSe	675.1 ± 7.4	4.52 ± 0.13	45.34 ± 0.29	1.39 ± 0.0575
TiO_2/C-dots	460.7 ± 36.1	0.19 ± 0.01	58.42 ± 3.26	0.05 ± 0.01
TiO_2/PbSe/CdS	691.4 ± 0.9	11.59 ± 0.34	43.98 ± 0.29	3.52 ± 0.14
TiO_2/PbSe/CdS/C-dots	690.1 ± 3.9	17.07 ± 0.19	41.10 ± 0.42	4.84 ± 0.13

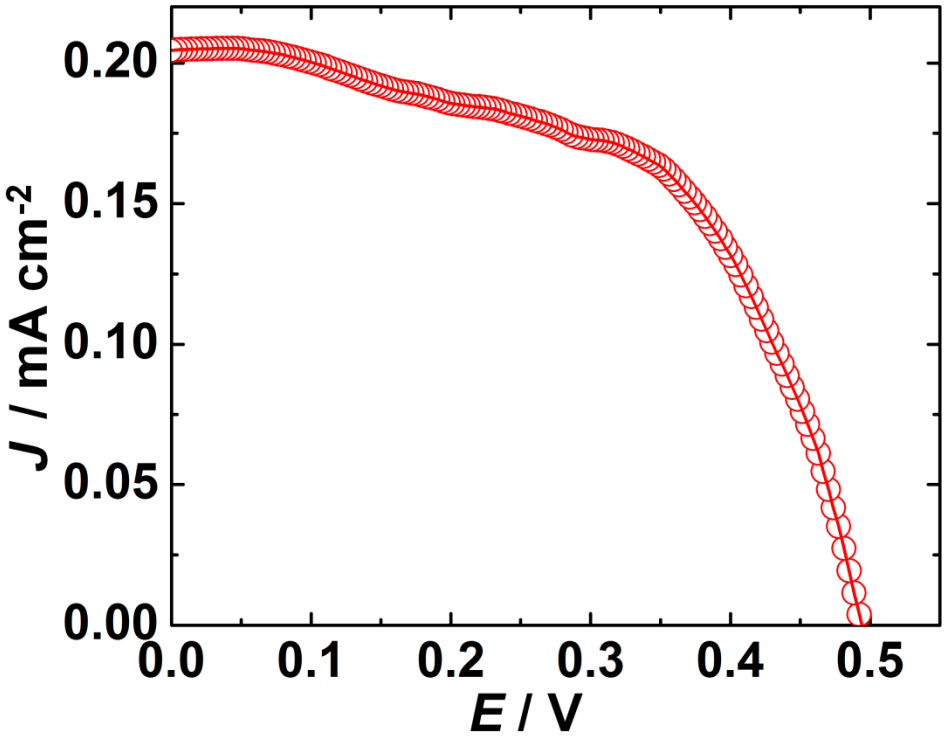

Figure S5 J-V characteristics of a cell with a TiO_2/C-dots electrode (①) as the photoanode under 1 sun illumination (AM 1.5G). A 0.1 M Na_2S solution in 3:7 (v/v) water:MeOH served as the electrolyte and a MWCNT/FTO assembly was used as the counter electrode.

The integrated area under the EQE (or IPCE) curve is a measure of J_{SC} and we find that the EQE values are under-estimated compared to the J_{SC} values obtained from J-V studies. The reason for this difference is the difference in the light intensity power (mW cm^{-2}) used for the two measurements in our case. For J-V measurements, a standard light source was used. We used a class AAA Newport-Oriel Solar Simulator, capable of providing a collimated light beam with an output of $\lambda > 300$ nm, with a power output of 100 mW cm^{-2} (1.5G Airmass filter). The term: "$\lambda > 300$ nm", implies that the light beam which impinges on the sample (of intensity of 1 Sun or 100 mW cm^{-2}) encompasses all wavelengths above 300 nm. This standard spectral output of the simulator was obtained from Newport. The system is equipped with a 450 W Xenon arc lamp, as the light source and Keithley 2420 digital source meter for J-V measurements. The spatial uniformity of irradiance was confirmed by us by calibrating with a 2 cm × 2 cm Si Reference Cell traceable to NREL and re-affirmed with a Newport power meter. On the other hand, for EQE or IPCE measurements, we used a Quantum Efficiency Measurement System, Oriel IQE-200™ capable of measurements compliant to ASTM E1021-06. This instrument gave the EQE and IQE values as a function of wavelength directly. But the light intensity (or power in mW cm^{-2}), which impinges upon a given sample at a given wavelength is much lower than what falls upon the sample (though integrated) in J-V measurements. We confirmed this by measuring the light intensity as a function of wavelength in the 300 to 1100 nm wavelength range for the system used for measuring IPCE values. The light intensities were measured at intervals of 10 nm, using a LOT-Oriel Radiometer-Photometer (model no. ILT 1400, 1G, 1000 W QTH), traceable to NIST. The spectrum is shown below. It is obvious from the profile of the light spectrum, that it is not similar to the spectrum of light (as in J-V measurements). The intensity of light is much lower in the entire spectral range (for the IPCE measurement system), and the difference is highly pronounced in the red/NIR region. Further, the spectral light irradiance offered by the simulator in J-V measurements is 100 mW cm^{-2} (calibrated with a standard reference Si solar cell), and in comparison, when we integrated the light curve for the IPCE measurement system, the net integrated light intensity is 39.6 mW cm^{-2}. A one-to-one comparison between J_{SC} from IPCE and J-V measurements is valid only if the integrated light intensities used for both measurements are equal (i.e. ideally, 100 mW cm^{-2}). As a consequence of this light intensity difference, in our case, the number of photons (of a monochromatic

wavelength) impinging upon the cell, are lesser than the required flux, and therefore the EQE or IPCE values are under-estimated.

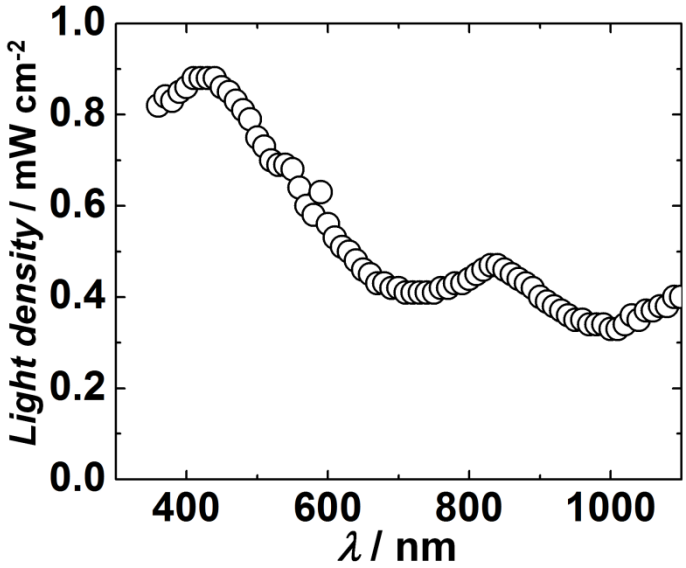

Figure S6 Spectral output from a QE measurement system (measured using a LOT-Oriel radiometer-photometer).

Table S3 Stability test for cells based on TiO_2/PbSe/CdS/C-dots, containing 0.1 M Na_2S as electrolyte and a MWCNTs/FTO as the counter electrode (under 1 sun illumination

Photoanode	V_{OC} (mV)	J_{SC} (mA cm^{-2})	FF	η (%)
TiO_2/PbSe/CdS/C-dots (As-fabricated)	694	17.26	41.52	4.97
TiO_2/PbSe/CdS/C-dots (4.97% Cell: After exposure to discontinuous 1 sun illumination for 3 h)	642	14.2	42.12	3.84
TiO_2/PbSe/CdS/C-dots (3.84% Cell: After storage in dark for 1 month)	615	10.26	39.27	2.48

Table S4 EIS fitting parameters for QDSCs (data from Figure 6)

Photoanode	R_{CE} (Ω)	R_{ct} (Ω)	C_{dl} (μF)	Y_o ($S\ s^{-1/2}$)
TiO_2/CdS	41.5	2800	8.65×10^{-5}	9.9×10^{-4}
TiO_2/PbSe	101	1530	1.0×10^{-4}	---
TiO_2/C-dots	4.2	103	1.71×10^{-2}	---
TiO_2/CdS/C-dots	23.5	455.7	8.3×10^{-5}	1.4×10^{-2}
TiO_2/PbSe/CdS/C-dots	21	134	7.5×10^{-5}	6.8×10^{-3}

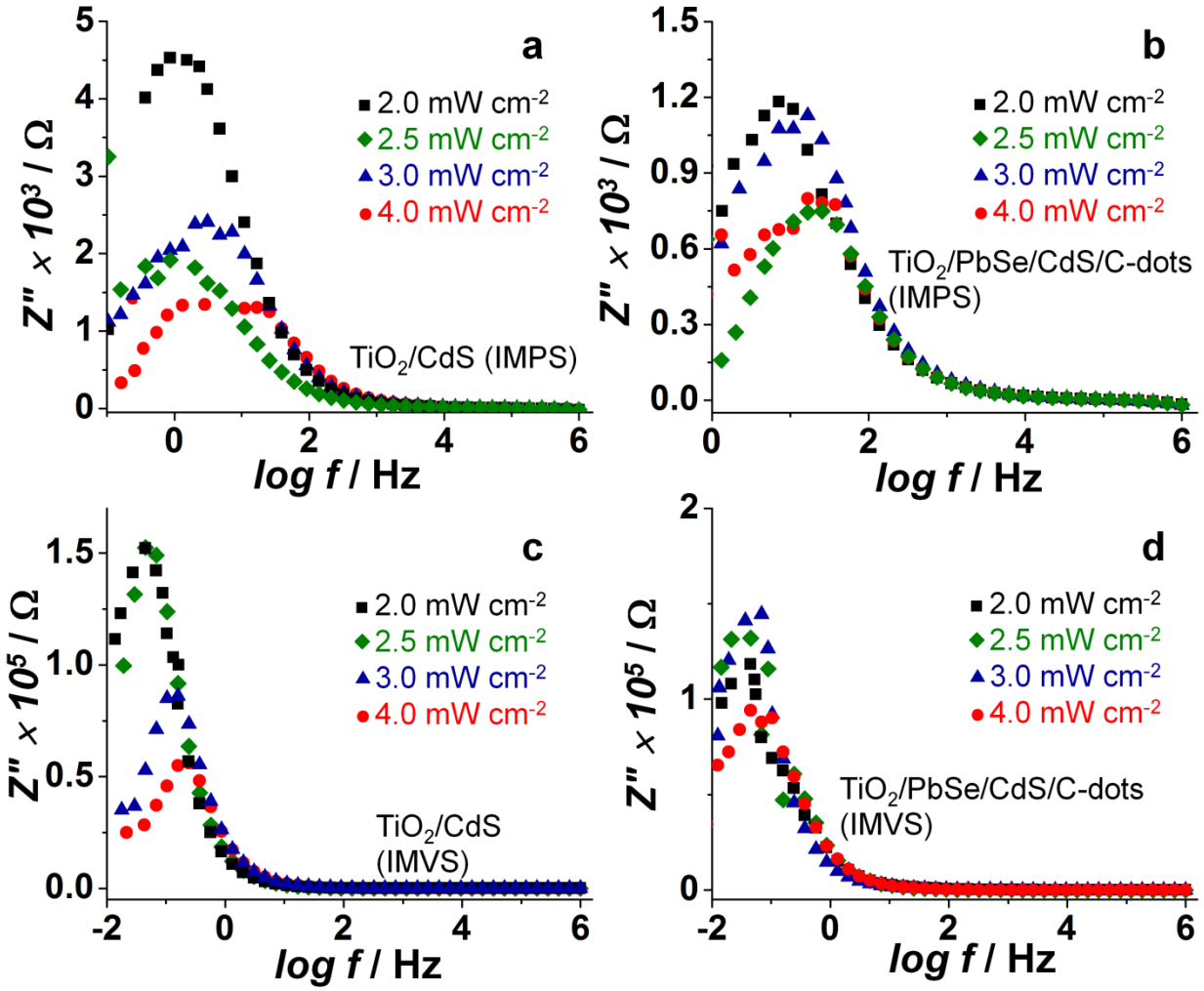

Figure S7 Imaginary components (of IMPS and IMVS) versus log (frequency) obtained under different light densities for: (a) TiO_2/CdS and (b) TiO_2/PbSe/CdS/C-dots based cells, via IMPS measurements and (c) TiO_2/CdS and (d) TiO_2/PbSe/CdS/C-dots based cells, via IMVS measurements.